DOI: 10.1534/genetics.109.107813

Suppression of Mitochondrial DNA Instability of Autosomal Dominant Forms of Progressive External Ophthalmoplegia-Associated *ANT1* Mutations in *Podospora anserina*

Riyad El-Khoury* and Annie Sainsard-Chanet*,†,[1]

**Centre National de la Recherche Scientifique (CNRS), Centre de Génétique Moléculaire, Gif-sur-Yvette F-91198, France and* †*Université Paris-Sud, Orsay F-91405, France*

Manuscript received July 28, 2009
Accepted for publication August 9, 2009

ABSTRACT

Maintenance and expression of mitochondrial DNA (mtDNA) are essential for the cell and the organism. In humans, several mutations in the adenine nucleotide translocase gene *ANT1* are associated with multiple mtDNA deletions and autosomal dominant forms of progressive external ophthalmoplegia (adPEO). The mechanisms underlying the mtDNA instability are still obscure. A current hypothesis proposes that these pathogenic mutations primarily uncouple the mitochondrial inner membrane, which secondarily causes mtDNA instability. Here we show that the three adPEO-associated mutations equivalent to A114P, L98P, and V289M introduced into the *Podospora anserina ANT1* ortholog dominantly cause severe growth defects, decreased reactive oxygen species production (ROS), decreased mitochondrial inner membrane potential ($\Delta\psi$), and accumulation of large-scale mtDNA deletions leading to premature death. Interestingly, we show that, at least for the adPEO-type M106P and A121P mutant alleles, the associated mtDNA instability cannot be attributed only to a reduced membrane potential or to an increased ROS level since it can be suppressed without restoration of the $\Delta\psi$ or modification of the ROS production. Suppression of mtDNA instability due to the M106P and A121P mutations was obtained by an allele of the *rmp1* gene involved in nucleo-mitochondrial cross- talk and also by an allele of the *AS1* gene encoding a cytosolic ribosomal protein. In contrast, the mtDNA instability caused by the S296M mutation was not suppressed by these alleles.

THE maintenance and expression of mitochondrial DNA (mtDNA) depend on many nuclear-encoded gene products. Recent studies have shown that defects in this maintenance can have devastating consequences for the cell and the organism. In humans, these defects are an important cause of neurological diseases including autosomal dominant (or recessive) progressive external ophthalmoplegia (adPEO) (Chinnery 2003; Copeland 2008). These disorders are characterized by multiple large-scale deletions of mtDNA. Three different genes that can cause PEO with multiple mtDNA deletions have been identified: the mtDNA polymerase (POLG), the heart/muscle isoform of the adenine nucleotide translocator (ANT1), and the mitochondrial DNA helicase, Twinkle.

The adenine nucleotide translocator (ANT), also known as the ADP/ATP mitochondrial translocator, is the most abundant protein in the inner mitochondrial membrane (Riccio *et al.* 1975; Nury *et al.* 2006; Klingenberg 2008). It exports ATP produced by mitochondrial oxidative phosphorylation toward the cytosol to meet the energy requirements of the cell; in exchange, it transports ADP into the mitochondrial matrix to fuel the conversion of ADP to ATP by the F_1F_O-ATP synthase. In humans, four isoforms of the ANT protein exist, and they are differently expressed in a tissue-specific manner (Stepien *et al.* 1992; Palmieri 2004; Dolce *et al.* 2005). The human ANT1 isoform is predominantly expressed in skeletal and cardiac muscle, and specific ANT1 mutations are associated with adPEO characterized by mtDNA instability (Kaukonen *et al.* 1999, 2000; Napoli *et al.* 2001; Komaki *et al.* 2002; Siciliano *et al.* 2003). In mice, *Ant1* knockout induces mitochondrial myopathy (Graham *et al.* 1997), increased H_2O_2 production, and mtDNA damage and inhibits oxidative phosphorylation (Esposito *et al.* 1999). Some of these mutations were introduced in the *AAC2* gene of *Saccharomyces cerevisiae* that encodes the major ADP/ATP mitochondrial translocator isoform in this organism. Numerous and sometimes contradictory effects have been reported depending in particular on the yeast laboratory strains examined (Kaukonen *et al.* 2000; Chen 2002, 2004; Fontanesi *et al.* 2004; Palmieri *et al.* 2005; Wang *et al.* 2008b).

In an attempt to better understand how these mutations affect mitochondrial DNA stability and their functional consequences on mitochondrial metabolism, we decided to introduce them in the unique ADP/ATP

Supporting information is available online at http://www.genetics.org/cgi/content/full/genetics.109.107813/DC1.

[1]*Corresponding author:* Centre de Génétique Moléculaire du CNRS, Allée de la Terrasse, Gif-sur-Yvette F-91198, France.
E-mail: annie.sainsard@cgm.cnrs-gif.fr

translocator gene of *Podospora anserina*, *PaAnt*. Like *S. cerevisiae*, the filamentous fungus *P. anserina* is an excellent system for genetic and molecular analyses. In contrast to *S. cerevisiae*, it is a strict multicellular aerobe that can display heteroplasmic states in which intact and rearranged mitochondrial genomes coexist. In this organism, life span is a reflection of mtDNA stability, and death is always associated with large mtDNA rearrangements. "Natural death" or aging is accompanied by large-scale reorganizations of the mtDNA whereas a nuclear-controlled premature death syndrome is accompanied by the accumulation of site-specific mtDNA deletions (Belcour *et al.* 1999; Silar *et al.* 2001 for reviews). *P. anserina* therefore occupies an interesting position among model systems for studying the cellular consequences of mutations in the ADP/ATP translocase gene.

We show here that the mutations M106P, A121P, and S296M, equivalent to the L98P, A114P (familial), and V289M (sporadic) human mutations, severely impair the vegetative and sexual development of the fungus and are responsible for decreased ROS production and for decreased inner membrane potential ($\Delta\psi$). The severity of the phenotypes differs according to the mutation. The three mutations show mtDNA instability, which leads to premature death. All these mutated traits are dominant. Interestingly, the mtDNA instability associated with the M106P and A121P mutations depends on the *rmp1* gene. This gene exists under two naturally occurring alleles, *rmp1-1* and *rmp1-2*, which control mtDNA integrity in some genetic contexts (Belcour *et al.* 1991; Contamine *et al.* 1996, 2004). When associated with the *rmp1-1* allele, the M106P and A121P mutations lead to rapid mtDNA instability whereas, in the presence of the *rmp1-2* allele, mtDNA instability is suppressed, and life span is considerably increased. Surprisingly, suppression is not accompanied by a restoration of the $\Delta\psi$ or a modification in the ROS level, demonstrating that these parameters are not sufficient to explain the M106P and A121P mtDNA instability. Mitochondrial DNA instability due to the M106P and A121P mutations is also suppressed by a mutation in the *AS1* gene encoding a ribosomal protein. The suppressor effects are not observed for the S296M mutation.

MATERIALS AND METHODS

***P. anserina* strains, growth conditions, life-span measurements, and transformation experiments:** The genetics and biological properties of *P. anserina* have been described and reviewed (Esser 1974). Strains used in this study were derived from the *s* wild-type strain (Rizet 1952). The *aox::hygro* (Δ*aox*) strain is inactivated for the endogenous *aox* gene (Lorin *et al.* 2001). The wild-type strain carrying an ectopic copy of the *rmp1-1* allele associated with a hygromycin-resistance cassette was described previously (Contamine *et al.* 2004). The *AS1-4* mutation was selected as an informational antisuppressor. Cultures were grown on standard minimal synthetic (M2) medium (Esser 1974) at 27°. When necessary, hygromycin 100 μg/ml (Boehringer-Mannheim), phleomycin 10 μg/ml (Boehringer-Mannheim), or nourseothricin 50 μg/ml (Werner BioAgents) were added to the medium. Medium for germination contains ground cornmeal (50 g/liter), agar (12.5 g/liter), and ammonium acetate (6 g/liter).

Life spans were measured on M2 medium in race tubes at 27° in the dark for three to five subcultures derived from 5 to 10 independent spores of a given strain. The life span of a strain is defined as the mean time (given with standard errors) of the growth of parallel cultures between the inoculation and the death of the culture. Protoplast preparation and transformation experiments were conducted as described previously (Bergès and Barreau 1989; El-Khoury *et al.* 2008).

Site-directed mutagenesis and gene replacement: The *PaAnt*$^+$ gene was cloned in pUC19 and then digested with *Sma*I to give a 4.2-kb *Sma*I restriction fragment, which was then introduced into the plasmid pAPI508, conferring resistance to nourseothricin to give pAPI-*PaAnt*$^+$ (El-Khoury *et al.* 2008), and into pBCHygro, conferring resistance to hygromycin (Silar 1995) to give pBC-*PaAnt*$^+$. pAPI-*PaAnt*$^+$ was then used as a template for mutagenesis of the *PaAnt*$^+$ gene by the QuikChange site-directed mutagenesis kit (Stratagene). The list of base changes and corresponding modified primers used to generate them is given in the supporting information, Table S1. After mutagenesis, the different constructs were sequenced to verify the presence of the correct base change. The resulting plasmids were used to replace the endogenous *PaAnt*$^+$ as described previously (El-Khoury *et al.* 2008). The pBC-*PaAnt*$^+$ plasmid was used to introduce by transformation an ectopic *PaAnt*$^+$ copy into the wild- type strain to obtain the *PaAnt*$^+$ (*PaAnt*$^+$) strain.

To delete the *PaAnt*$^+$ gene, targeting fragments of 1.3 kb (5′) and 1.1 kb (3′) flanking the *PaAnt* gene were prepared by PCR on genomic DNA using the primer pairs E-5′-UTR (5′-TCGAATTGGAGTTGGGAAAG-3′) and S-5′-UTR (5′-GTC AGCCACAGCAAGATGAA-3′) and N-3′-UTR (5′-GGATCAGA GGCTTCATCGTC-3′) and S-3′-UTR (5′-TGACAACCCAGGT TCTTTGA-3′), respectively. The two fragments bear *Eco*RI–*Spe*I and *Not*I–*Spe*I restriction sites and were introduced sequentially into the corresponding sites of the polylinker of plasmid pPable that contains a phleomycin- resistance cassette (Coppin and Debuchy 2000). The resulting vector, pPable-Δ*PaAnt*$^+$, was digested by *Spe*I, and ~10 μg of linear plasmid was used to transform the *PaAnt*$^+$ *(PaAnt*$^+$*)* strain. The deletion of the endogenous *PaAnt*$^+$ gene was verified by PCR and Southern blot.

Mitochondrial DNA analysis: The mtDNA of the different growing or dying cultures was extracted by minipreparation (Lecellier and Silar 1994). The probes used in this study were *Eco*IV, *Eco*I, and 2604 (described previously by Begel *et al.* 1999); they cover ~80% of the mitochondrial genome.

Western blot: Mitochondria were isolated as previously described (Sellem *et al.* 2007). Thirty micrograms of mitochondrial protein were fractionated by SDS–PAGE and transferred to a nitrocellulose membrane. Immunochemistry was performed with an anti-Aac2 monoclonal antibody generated against the Aac2 protein of *S. cerevisiae*. This antibody, kindly donated by E. Kunji, was raised against the Aac2 conserved motif SYPLDTVRRRMMMT (Bamber *et al.* 2007). In addition, blots were reprobed with an anti-βATPase antibody (a gift from J. Velours) as a standardization control. The bound antibodies were detected using an enhanced chemiluminescence detection system (Pierce Supersignal West picochemiluminescent substrate).

Quantitative RT–PCR: Total RNA was extracted using the RNeasy plant mini kit (Qiagen) from cultures grown for 48 hr on cellophane disks overlying M2 medium. The mycelium was

broken with glass beads in a Fastprep apparatus (40 sec, intensity 6.5). For quantitative RT–PCR (qRT–PCR), cDNA was synthesized with SuperScript II reverse trancriptase (Invitrogen) from 2 μg of RNA, using a T_{15} primer. Subsequent quantitative real-time PCRs were performed in a Lightcycler (Roche), using the LightCycler FastStart DNAMaster SYBR Green I kit (Roche). At least three independent experiments were performed on one to three different RNA preparations for each strain. Primers QAOX4-F (5′-TGATCTCGCCACG AATTACA-3′) and QAOX4-R (5′-TATAGGTGTGGACCGCT TCC-3′) were used for the *aox* gene.

Mitochondrial morphology: The wild type, $PaAnt^{M106P}$, $PaAnt^{A121P}$, and $PaAnt^{S296M}$ strains were crossed with a strain that carries the pAPI213 transgene consisting of the mitochondrial targeting sequence of the *Neurospora crassa atp9* gene cloned in frame with the enhanced green fluorescent protein (EGFP) sequence and a hygromycin- resistance cassette (Sellem *et al.* 2007) Wild-type and mutant strains expressing this transgene were obtained. They were grown on thin synthetic solid medium for 12–24 hr. The area of medium containing the mycelium was cut out and transferred onto a microscopic slide. Fluorescence was observed with a Zeiss Axioplan 2 upright microscope equipped with a photometrics CoolSnap HQ (Roper Scientific) camera and Metamorph software.

Respiration analysis: The rate of respiration was estimated *in vivo* in an oxytherm chamber with a Clark-type O_2 electrode (Hansatech), using mycelia grown on cellophane disks overlying M2 medium for 48 hr or using protoplast suspensions (3.10^7 protoplasts/ml in 0.6 M sucrose). Cyanide (KCN, 1 mM) was added to inhibit the cytochrome pathway.

Flow cytometry, ROS, and mitochondrial membrane potential ($\Delta\psi$) measurements: ROS elimination was measured by the production of dichlorofluorescin (DCF) resulting from the oxidation of the diacetate form (H_2DCF-DA). For each strain, 10^7 protoplasts were incubated in H_2DCF-DA (80 μM in 0.4 M sucrose/50 mM phosphate buffer, pH 6), and measurements of the fluorescent DCF were performed after 90 min. The cytometric measurements were performed in a Partec PAS-III flow cytofluometer. Mitochondrial membrane potential ($\Delta\psi$) was measured by incubating protoplasts (10^6/ml) in 0.1 μM of 3,3′-dihexyloxacarbocyanine iodide [$DiOC_6(3)$] (Sigma Aldrich) for 30 min at 25°. Protoplasts were centrifuged to remove the excess fluorochrome and resuspended in fresh medium before analysis. Control samples were prepared with 17 μM final carbamoyl cyanide *m*-chlorophenylhydrazone (mClCCP), an ionophore that dissipates the mitochondrial membrane potential. This drug was added to the protoplasts 15 min before $DiOC_6(3)$. Fluorescence of the $DiOC_6(3)$ was measured in a Partec PAS-III flow cytofluometer.

Nonyl-acridine orange, MitoFluor Green, and MitoTracker Green were not suitable for the quantification of mitochondria because we observed that their accumulation in the mitochondria is dependent on the membrane potential in *P. anserina* (data not shown); therefore, the fluorescence values of $DiOC_6(3)$ were normalized using the quantity of mitochondrial protein determined by the Bradford method (Bio-Rad).

RESULTS

The genome of *P. anserina* encodes a unique *PaAnt* gene whose deletion is lethal: Taking advantage of the recently sequenced genome of *P. anserina* (Espagne *et al.* 2008), we identified a unique gene (*PaAnt*) encoding a homolog of the human ANT1 protein. The 315-amino-acid protein deduced from the *PaAnt* sequence shares 71.3%, 47.3%, and 48.3% identity with Aac2, ADT1, and hANT1 proteins from *S. cerevisiae*, *Bos taurus*, and *Homo Sapiens*, respectively (Figure S1). The *PaAnt* gene was cloned and modified as described in materials and methods. It was first deleted in a strain bearing an ectopic copy (*PaAnt*$^+$*-Hygro*) of the wild-type gene. The primary transformants *PaAnt::Phleo* (*PaAnt*$^+$*-Hygro*) were crossed with a wild-type strain. The analysis of >50 asci clearly revealed that all the homocaryotic spores resistant to phleomycin and sensitive to hygromycin were unable to germinate, indicating that the *PaAnt::Phleo* genotype is viable only when the ectopic transgene is present. This allows us to conclude that the inactivation of the *PaAnt* gene is lethal for *P. anserina* and to confirm that no functionally redundant gene is present in the genome.

***PaAnt* alleles equivalent to *hANT1* mutants responsible for adPEO cause pleiotropic somatic and sexual defects:** To mimic the L98P, A114P, and V289M human mutations responsible for adPEO, the corresponding Met106, Ala121, and Ser296 codons of the *P. anserina* ANT protein were changed to proline, proline and methionine codons, respectively (Figure S1). The three mutant alleles $PaAnt^{M106P}$, $PaAnt^{A121P}$, and $PaAnt^{S296M}$ were introduced site specifically in place of the endogenous wild-type gene as previously described (El-Khoury *et al.* 2008). The recipient strain used for the transformation-mediated gene replacement carried an ectopic wild-type allele. The primary transformants were crossed with wild type. Monocaryotic spores bearing a mutated allele (determined by resistance to nourseothricin) without the ectopic $PaAnt^+$ allele (determined by the hygromycin sensitivity) were obtained for the three mutations, revealing that none of them is lethal. Thus, we obtained $PaAnt^{M106P}$, $PaAnt^{A121P}$, and $PaAnt^{S296M}$ strains in which the mutated allele is subject to the normal regulatory control of the *PaAnt* gene. The three mutant strains displayed drastic phenotypic alterations. They showed a delayed and reduced rate of germination, a slow vegetative growth rate (Table 1A), a heterogeneous mycelial aspect with very pigmented sectors devoid of aerial hyphea (Figure 1), female sterility, and reduced male fertility (data not shown).

The three *PaAnt* mutations cause a strong decrease of mtDNA stability and life span, which are suppressed for M106P and A121P but not S296M by the *rmp1-2* allele: The three *hANT1* mutations leading to PEO disease are associated with multiple deletions of the mitochondrial genome in skeletal muscle. In *P. anserina*, life span is an indicator of mtDNA stability. Life span and death-associated mtDNA instability were therefore analyzed in the three strains $PaAnt^{M106P}$, $PaAnt^{A121P}$, and $PaAnt^{S296M}$. Surprisingly, as shown in Table 1A, except for the $PaAnt^{S296M}$ mutant that showed a premature death phenotype whatever the mating type (~5– 6 days compared to 18 days for the wild-type strain), the life span of the $PaAnt^{M106P}$ and $PaAnt^{A121P}$ mutants was severely reduced (~2 fold) or greatly increased (>10- fold)

TABLE 1

Growth rate and life span of strains carrying different *PaAnt* mutant alleles

Strain	Growth rate (mm/day ± SE)	Life span (days ± SE)
A		
PaAnt^{+}, *rmp1-2 mat+*	6.5 ± 0.2	18.2 ± 1.2
PaAnt^{+}, *rmp1-1 mat−*	6.7 ± 0.1	17.7 ± 0.8
PaAnt^{M106P}, *rmp1-2 mat+*	4 ± 0.2	>180
PaAnt^{M106P}, *rmp1-1 mat−*	3.6 ± 0.4	9.4 ± 2.1
PaAnt^{A121P}, *rmp1-2 mat+*	5.2 ± 0.1	>180
PaAnt^{A121P}, *rmp1-1 mat−*	4.9 ± 0.4	9.4 ± 1.1
PaAnt^{S296M}, *rmp1-2 mat+*	4.2 ± 0.4	5.6 ± 1
PaAnt^{S296M}, *rmp1-1 mat−*	4.5 ± 0.7	5.8 ± 0.7
B		
PaAnt^{M106P}, *rmp1-2 mat+ (rmp1-1)*	ND	9.2 ± 1.4
PaAnt^{A121P}, *rmp1-2 mat+ (rmp1-1)*	ND	9 ± 2
C		
PaAnt^{M106P} (*PaAnt*$^{+}$) *rmp1-2 mat+*	4.7 ± 0.6	>180
PaAnt^{M106P} (*PaAnt*$^{+}$) *rmp1-1 mat−*	4.7 ± 0.2	11.3 ± 0.9
PaAnt^{A121P} (*PaAnt*$^{+}$) *rmp1-2 mat+*	5.3 ± 0.1	>180
PaAnt^{A121P} (*PaAnt*$^{+}$) *rmp1-1 mat−*	4.5 ± 0.1	11.4 ± 0.8
PaAnt^{S296M} (*PaAnt*$^{+}$) *rmp1-2 mat+*	4 ± 0.5	5.1 ± 1.3
PaAnt^{S296M} (*PaAnt*$^{+}$) *rmp1-1 mat−*	3.8 ± 0.2	5.2 ± 1.2

(A) Characteristics of the homoallelic strains carrying the wild-type or a mutant allele of *PaAnt* associated with *rmp1-1 mat−* or *rmp1-2 mat+*. (B) Characteristics of the *PaAnt*^{M106P} *rmp1-2 mat+* and *PaAnt*^{A121P} *rmp1-2 mat+* strains carrying an ectopic copy of the *rmp1-1* allele. (C) Characteristics of the heteroallelic strains carrying a mutant allele of *PaAnt* and an ectopic copy of the wild-type allele associated with *rmp1-1 mat−* or *rmp1-2 mat+*.

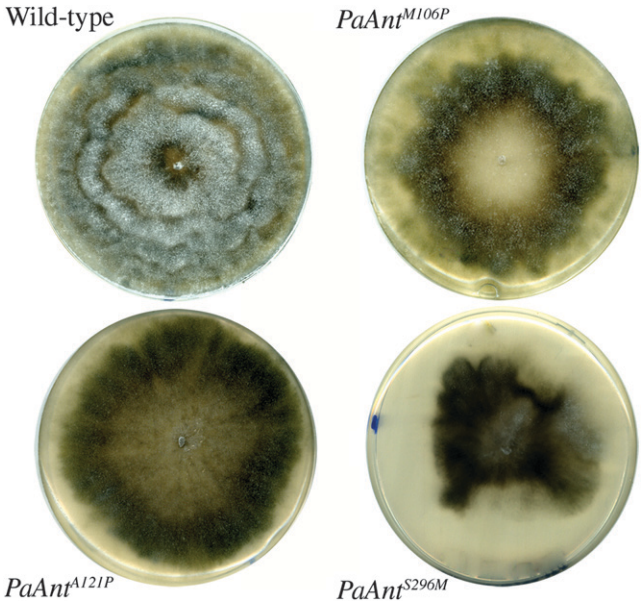

FIGURE 1.—Mycelium aspect of the wild type and the three *PaAnt* mutants. Petri plates of M2 medium were inoculated with an explant of each strain and incubated for 6 days at 27°. The wild type exhibits dense, aerial mycelium whereas the three mutants exhibit a heterogeneous mycelium with highly pigmented sectors devoid of aerial hyphae. The vegetative growth of the *PaAnt*^{S296M} strain stopped prematurely. The strains presented are all *rmp1-2 mat+*; the equivalent *rmp1-1 mat−* strains display similar phenotypes.

according to the mating type, *mat−* or *mat+*, respectively. The *mat−* cultures displayed a reduction in life span of ~2-fold whereas the *mat+* cultures displayed an increase in life span of >10-fold (>180 days). A gene, *rmp1*, exists as two naturally occurring alleles, *rmp1-1* and *rmp1-2*. This gene is tightly linked to the *mat* locus (*mat−* and *mat+*, respectively) and is involved in the timing of death in a certain genetic context (CONTAMINE *et al.* 1996). We asked whether, in the *PaAnt*^{M106P} and *PaAnt*^{A121P} strains, the differences in life span between the two *mat* loci revealed an interaction between the *PaAnt* gene and the *mat* locus or between the *PaAnt* gene and the *rmp1* gene. To address this question, we took advantage of a strain bearing an ectopic copy of the dominant *rmp1-1* gene (CONTAMINE *et al.* 2004) to introduce it by a genetic cross into the *PaAnt*^{M106P} and *PaAnt*^{A121P} *rmp1-2 mat+* strains. Interestingly, as shown in Table 1B, the introduction of *rmp1-1* into either *PaAnt*^{M106P} or *PaAnt*^{A121P} *rmp1-2 mat+* strains led to a premature death phenotype similar to that observed in *PaAnt*^{M106P} and *PaAnt*^{A121P} *rmp1-1 mat−* strains. This demonstrates that the timing of death in *PaAnt*^{M106P} and *PaAnt*^{A121P} mutants depends on the presence of the *rmp1-1* or the *rmp1-2* allele and not on the mating type.

In *P. anserina*, growth arrest of the wild-type strain by aging is correlated with the accumulation of short mtDNA sequences (senDNAs) as amplified circular multimeric molecules. Large amounts of senDNAα are systematically observed in senescent wild-type cultures (see BELCOUR *et al.* 1999 for review). In marked contrast to this situation, in the dying *PaAnt*^{M106P} *rmp1-1* and *PaAnt*^{A121P} *rmp1-1* cultures (Figure 2B), as in the dying *PaAnt*^{S296M} *rmp1-1* and *rmp1-2* cultures (Figure 3), death is not associated with the accumulation of senDNAα. The mtDNA profile of independent *PaAnt*^{M106P} *rmp1-1* and *PaAnt*^{A121P} *rmp1-1* cultures revealed large-scale rearrangements and the loss of numerous fragments covering ~60% of the wild-type chromosome (Figure 2B and Figure S2). These data were confirmed by the use of different probes covering ~80% of the mitochondrial genome. Remarkably, some of these fragments were systematically lost in independent cultures, indicating that the deletions cover a common region of the mitochondrial genome. However, different additional fragments presumed to result from circularization of the deleted chromosomes were recovered in the different dying cultures, indicating that these deletions are not site specific and present different boundaries. In contrast, the analysis of the mtDNA content of independent dying *PaAnt*^{S296M} *rmp1-1* or *rmp1-2* cultures revealed multiple rearrangements different from one culture to another and affecting different parts of the

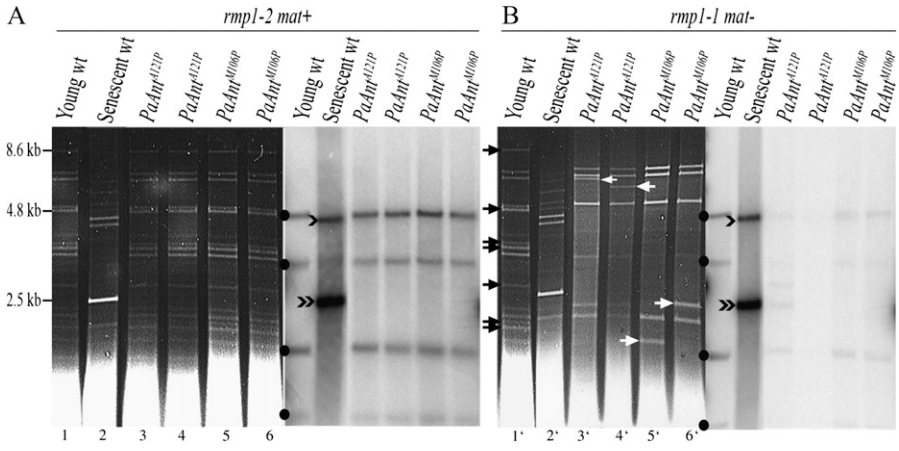

FIGURE 2.—Effects of *PaAnt*^{M106P} and *PaAnt*^{A121P} mutant alleles on mtDNA. (A) *rmp1-2 mat+* strains. (B) *rmp1-1 mat−* strains. (Left, A and B) The ethidium-bromide-stained *Hae*III restriction patterns of mtDNA extracted from different cultures. (Right, A and B) The corresponding Southern blots probed with a fragment of the *P. anserina* mitochondrial genome including the α-region. This probe reveals four fragments indicated by solid dots on intact mtDNA molecules. In senescent wild-type cultures, it reveals a fragment of 2.5 kb (indicated by a black double arrowhead) corresponding to senDNAα and a fragment of 5 kb (black arrowhead) potentially corresponding to a dimer of senDNAα. (A) Lane 1: young wild-type *rmp1-2 mat+* culture; lane 2: senescent wild-type *rmp1-2 mat+* culture; lanes 3 and 4: independent *PaAnt*^{A121P} *rmp1-2 mat+* cultures after 180 days of growth; lanes 5 and 6: independent *PaAnt*^{M106P} *rmp1-2 mat+* cultures after 180 days of growth. (B) Lane 1′: young wild-type *rmp1-1 mat−* culture; lane 2′: senescent wild-type *rmp1-1 mat−* culture; lanes 3′ and 4′: independent dying *PaAnt*^{A121P} *rmp1-1 mat−* cultures; lanes 5′ and 6′: independent dying *PaAnt*^{M106P} *rmp1-1 mat−* cultures. Black arrows indicate fragments present in the wild-type chromosome that are absent or underrepresented in the mtDNA from *PaAnt*^{M106P} *rmp1-1 mat−* and *PaAnt*^{A121P} *rmp1-1 mat−* cultures. White arrows indicate additional fragments presumed to correspond to deletion junctions.

mitochondrial genome (Figure 3). One interesting outcome of the mtDNA analysis (shown in Figure 2A) is that, whereas the *PaAnt*^{M106P} and *PaAnt*^{A121P} mutations are responsible for mtDNA instability in the presence of the *rmp1-1* allele as observed in adPEO patients, this instability is suppressed in the presence of the *rmp1-2* allele: the mtDNA of the long-lived *PaAnt*^{M106P} *rmp1-2 mat+* and *PaAnt*^{A121P} *rmp1-2 mat+* mutants remained stable for >180 days.

Western blot analyses were performed to determine whether a reduced amount of mutant protein could explain the phenotypic alterations of the mutants and the differences of mtDNA instability between the *PaAnt*^{M106P} and *PaAnt*^{A121P} strains harboring the *rmp1-1* or the *rmp1-2* allele. Only *PaAnt*^{M106P} and *PaAnt*^{A121P} mutants were studied because we were not able to prepare sufficient mitochondria from the *PaAnt*^{S296M} mutant due to its premature death phenotype. As shown on Figure 4, the amount of the mutant protein is reduced (~50% of wild type) in both the *PaAnt*^{M106P} and the *PaAnt*^{A121P} strain. However, no difference was observed in either *rmp1-1* or *rmp1-2* strains, indicating that the mtDNA instability is not correlated to a reduced protein content.

Mutation in a cytosolic ribosomal protein suppresses the premature death phenotype conferred by the mutations M106P and A121P but not S296M: In *S. cerevisiae*, it was recently shown that the *aac2*^{A128P} mutation leads to the formation of degenerative microcolonies whose frequency increases with age. This degenerative cell death is partially suppressed by reduced cytosolic protein synthesis (WANG *et al.* 2008a). In *P. anserina*, mutations that affect the translation apparatus drastically modify life span and mtDNA stability (SILAR *et al.* 2001). However, the nature of the relationships between protein synthesis, aging, and associated mtDNA instability are unclear. The most striking effect observed is that of the *AS1-4* mutation identified as affecting the fidelity of translation (COPPIN-RAYNAL 1981). This mutation is located in a cytosolic ribosomal protein (DEQUARD-CHABLAT and SELLEM 1994) that, in association with the *rmp1-1* or the *rmp1-2* alleles, drastically shortens or increases life span (BELCOUR *et al.* 1991; CONTAMINE *et al.* 1996). Interestingly, like the *PaAnt*^{M106P} and *PaAnt*^{A121P} strains, dying *AS1-4* cultures accumulate large

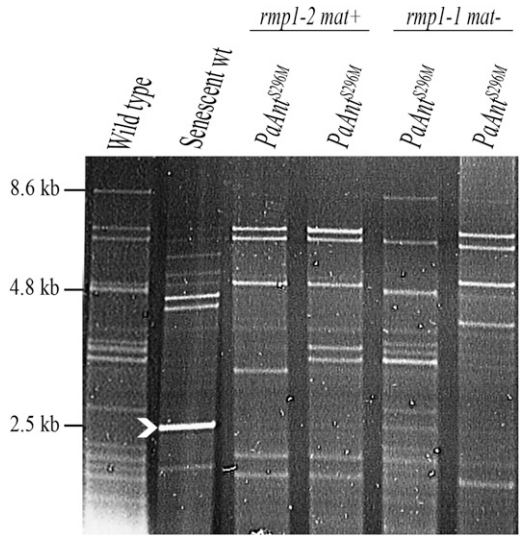

FIGURE 3.—Effects of the *PaAnt*^{S296M} mutant allele on mtDNA. Ethidium- bromide- stained *Hae*III restriction patterns of mtDNA extracted from different dying *PaAnt*^{S296M} cultures. The white arrowhead indicates the position of senDNAα.

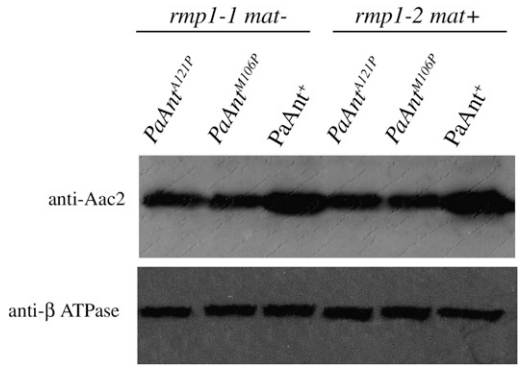

Figure 4.—Western blot analysis of the PaANT protein. Mitochondrial protein extracts (30 μg) from mitochondria extracted from the wild-type, *PaAnt*^{M106P}, and *PaAnt*^{A121P} strains (*rmp1-1 mat*− and *rmp1-2 mat*+) were separated on SDS–PAGE and probed with a yeast Aac2 monoclonal antibody. The blot was reprobed with an antibody directed against the β-subunit of ATPase as loading control.

mitochondrial deletions, but these are characterized by precise boundaries (Belcour *et al.* 1991; Sainsard-Chanet *et al.* 1998; Figure S2). To test whether the *AS1-4* mutation is able to suppress the premature death phenotype due to the *PaAnt* mutations, it was associated with the three *PaAnt*^{M106P}, *PaAnt*^{A121P}, and *PaAnt*^{S296M} mutations by crosses. Remarkably, the premature death phenotype and the mtDNA instability of *PaAnt*^{M106P} *rmp1-1* and *PaAnt*^{A121P} *rmp1-1* were suppressed in the presence of the *AS1-4* mutation, and a synthetic phenotype was obtained (life span >60 days) (Table 2). In contrast, the premature death of *PaAnt*^{S296M} *rmp1-1* and *rmp1-2* was not suppressed by *AS1-4*. Furthermore, whereas the life span of the *AS1-4 rmp1-2* strain was greatly increased, that of the double mutant *PaAnt*^{S296M} *AS1-4 rmp1-2* was very short, and the mtDNA pattern at the time of death corresponded to multiple rearrangements as in the *PaAnt*^{S296M} single mutant, indicating that *PaAnt*^{S296M} is epistatic to the *AS1-4* mutation. In the same way, the double mutants *PaAnt*^{M106P} *AS1-4* and *PaAnt*^{A121P} *AS1-4* shared the same mycelial aspect, female sterility, and growth rate as the single *PaAnt*^{M106P} and *PaAnt*^{A121P} mutants (Table 2), indicating that, although *AS1-4* suppresses the mtDNA instability, the translocase mutations are epistatic to the *AS1-4* mutation for the somatic and sexual defects.

The mutant *PaAnt* alleles lead to morphological alterations of mitochondria and reduction in respiratory activity, ROS production, and inner membrane potential: The effect of the different *PaAnt* mutations on mitochondrial structure and morphology was examined using a reporter system composed of the EGFP protein to which a mitochondrial-targeting presequence was added (Sellem *et al.* 2007). The construct was integrated after transformation into a wild-type strain and transferred into the three mutants through crosses. Whereas the wild-type strain contained long filamentous mitochondria, the mitochondrial structure of the mutants was considerably modified and fragmented (Figure 5). Interestingly, the mutants showed a similar mitochondrial phenotype regardless of the *rmp1* allele, life span, and mtDNA stability. The strongest phenotype was observed in *PaAnt*^{S296M}, in which the majority of mitochondria seemed to be organized in aggregates while, in *PaAnt*^{M106P} and *PaAnt*^{A121P}, they appeared as small fragmented filaments. These results indicate that the three *PaAnt* mutations affect mitochondrial structure and morphology.

TABLE 2

Suppression of the short-lived phenotype of *PaAnt*^{M106P} *rmp1-1* and *PaAnt*^{A121P} *rmp1-1* by the *AS1-4* mutation

Strain	Growth rate (mm/day ± SE)	Life span (days ± SE)
PaAnt^{+}, *AS1-4*, *rmp1-2 mat*+	5.6 ± 0.2	>100
PaAnt^{+}, *AS1-4*, *rmp1-1 mat*−	5.5 ± 0.1	~4
PaAnt^{M106P}, *AS1-4*, *rmp1-2 mat*+	4.5 ± 0.2	>60
PaAnt^{M106P}, *AS1-4*, *rmp1-1 mat*−	3.7 ± 0.4	>60
PaAnt^{A121P}, *AS1-4*, *rmp1-2 mat*+	4.4 ± 0.1	>60
PaAnt^{A121P}, *AS1-4*, *rmp1-1 mat*−	4.9 ± 0.1	>60
PaAnt^{S296M}, *AS1-4*, *rmp1-2 mat*+	4.2 ± 0.2	5.5 ± 0.8
PaAnt^{S296M}, *AS1-4*, *rmp1-1 mat*−	3.9 ± 0.3	6 ± 0.5

We then tested the effects of the *PaAnt* mutations on oxygen consumption, ROS production, and mitochondrial inner membrane potential (Δψ). Only *PaAnt*^{M106P} and *PaAnt*^{A121P} mutants (both the long-lived *rmp1-2 mat*+ and the short-lived *rmp1-1 mat*− strains) were studied because we were not able to prepare sufficient protoplasts from the *PaAnt*^{S296M} mutant as previously mentioned. As shown in Table 3, the respiratory activity of the *PaAnt*^{M106P} and *PaAnt*^{A121P} mutants, regardless of the *rmp1* allele, life span, and mtDNA stability, was decreased by a factor of 2–3 compared to that of wild type. Furthermore, in contrast to the wild-type strain in which oxygen consumption is very sensitive to cyanide, respiration was ~50% resistant to cyanide in the two mutants. In *P. anserina*, resistance to cyanide has previously been reported in several respiratory mutants partially or completely deficient for complexes III or IV and is due to the induction of an alternative oxidase (AOX) (Dufour *et al.* 2000; Stumpferl *et al.* 2004; Sellem *et al.* 2007). Quantitative RT–PCR experiments revealed that the amount of *aox* transcripts increased ~7- to 20-fold in the mutants compared to the wild type (Table 3). The induction of the alternative oxidase and the reduction of cellular respiration in the *PaAnt*^{M106P} and *PaAnt*^{A121P} strains strongly suggest that these mutations cause damage to the cytochrome part of the electron transport chain. However, as the strains display similar respiratory properties whatever their mtDNA stability, this damage is probably independent of the mtDNA instability.

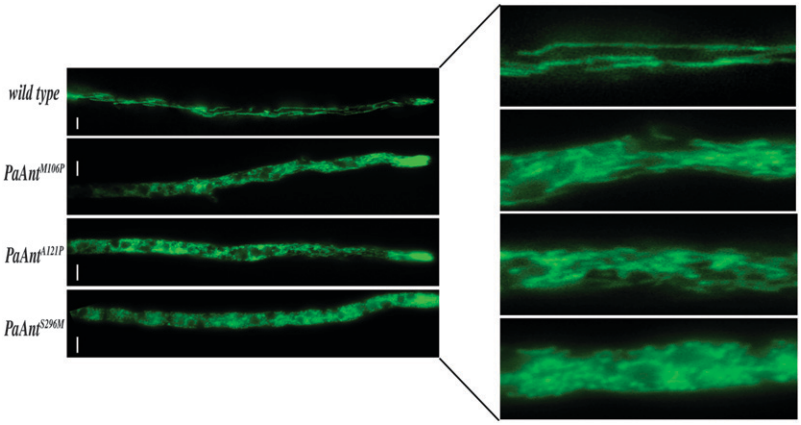

FIGURE 5.—Analysis of mitochondrial morphology in wild type, *PaAnt*^{M106P}, *PaAnt*^{A121P} and *PaAnt*^{S296M} strains. (Right) An enlargement of a sector of the filaments. The wild-type strain shows snakelike mitochondria. The *PaAnt*^{M106P} and *PaAnt*^{A121P} mutants show fragmented filamentous mitochondria, and the *PaAnt*^{S296M} mutant shows aggregated mitochondria. The represented strains are *rmp1-2 mat+*. *The rmp1-1 mat–* strains display similar phenotypes. Bars, 5 μm.

We then analyzed the effects of the *PaAnt*^{M106P} and *PaAnt*^{A121P} mutations on ROS production by flow cytofluometry, by incubating protoplasts with H_2DCF-DA, and by monitoring the formation of fluorescent DCF. In both *PaAnt*^{M106P} and *PaAnt*^{A121P} mutants, regardless of the *rmp1* allele, life span, and mtDNA stability, the intensity of fluorescence was about three fold less than in the wild type, indicating a clear decrease in ROS production in these mutants (Table 3). To investigate if the reduced levels of ROS could be explained by the expression of the alternative oxidase known to act in some situations as an antioxidant enzyme (MAXWELL *et al.* 1999), the *PaAnt*^{M106P} and *PaAnt*^{A121P} mutant strains devoid of the *aox* gene (obtained after crosses with the Δ*aox* strain) were also analyzed. As shown in Table 3, the ROS production and respiration rate were similar in *PaAnt*^{M106P} and *PaAnt*^{A121P} strains whether the *aox* gene was expressed or inactivated. This result demonstrates that the reduction of ROS production is not due to the presence of the alternative oxidase but rather to the reduced respiratory activity of the mutants. We also measured the expression levels of the *PaSod3* and *PaSod1* genes encoding the mitochondrial and cytosolic superoxide dismutases, respectively (BORGHOUTS *et al.* 2002), by qRT–PCR in the *PaAnt*^{M106P}, *PaAnt*^{A121P}, and wild-type strains. These levels were not significantly different between the genotypes (data not shown), which is consistent with the absence of oxidative stress in the *PaAnt* mutants studied. This result is important; it indicates that (1) the life span of the strains carrying the adPEO alleles is not correlated to the ROS level and (2) the mitochondrial instability of the *PaAnt rmp1-1* mutant strains is not associated with increased mitochondrial oxidative stress.

TABLE 3

Mitochondrial characteristics of strains carrying different *PaAnt* mutant alleles

Strain	Respiration rate (nmol $O_2 \cdot min^{-1}$)	KCN inhibition level (%)	Relative abundance of AOX transcripts	ROS production level	Membrane potential level (Δψ)	Δψ + mClCCP
PaAnt^{+}, *rmp1-2 mat+*	25.9 ± 3.2	83	1	93 ± 6	35 ± 3	7.66 ± 0.2
PaAnt^{+}, *rmp1-1 mat–*	22.1 ± 4.1	88	1	99 ± 2	33 ± 2.8	7 ± 0.2
PaAnt^{M106P}, *rmp1-2 mat+*	9.8 ± 0.7	58	7.5 ± 0.9	37.6 ± 2	16 ± 1.1	7.3 ± 0.3
PaAnt^{M106P}, *rmp1-1 mat–*	9.3 ± 2.2	62	23 ± 8	42.5 ± 3.5	14.3 ± 1.2	7.4 ± 0.3
PaAnt^{A121P}, *rmp1-2 mat+*	12.8 ± 2.1	33	7 ± 0.8	34.9 ± 3	16 ± 1.2	4 ± 0.3
PaAnt^{A121P}, *rmp1-1 mat–*	8.2 ± 0.9	56	9.5 ± 1	39 ± 2	14.9 ± 1.2	4.2 ± 0.2
PaAnt^{+}, Δ*aox*, *rmp1-2 mat+*	24.3 ± 3.3	95	—	81.5 ± 4	—	—
PaAnt^{M106P}, Δ*aox*, *rmp1-2 mat+*	10.2 ± 1.6	94	—	36.1 ± 2.2	—	—
PaAnt^{A121P}, Δ*aox*, *rmp1-2 mat+*	8.7 ± 1.4	94	—	39 ± 2	—	—
PaAnt^{+} (*PaAnt*$^{+}$), *rmp1-2 mat+*	24.3 ± 0.8	—	—	96 ± 3.6	34.8 ± 3.1	8.9 ± 0.6
PaAnt^{M106P} (*PaAnt*$^{+}$), *rmp1-2 mat+*	14.3 ± 0.4	—	—	40 ± 1.7	11.1 ± 1.8	4.3 ± 0.7
PaAnt^{A121P} (*PaAnt*$^{+}$), *rmp1-2 mat+*	12.3 ± 0.8	—	—	44 ± 3.3	15.1 ± 1	5.1 ± 1.9

Respiration rate was measured on 3.10^7 protoplasts for each experiment and expressed as nanomoles min^{-1} ± SE. The relative abundance of the *aox* transcripts was measured by real-time qPCR experiments. For each strain, the level of the *aox* transcripts was normalized using the *gpd* transcript level, which was used as a standard; the *aox* mRNA copy number was given a value of 1 in the wild-type strain. ROS and Δψ measurements were carried out on protoplasts in a Partec PAS-III flow cytofluometer. The values correspond to the mean fluorescent intensity of the fluorescent probes H_2DCF-DA (80 mM) and $DIOC_6(3)$ (0.1 mM) used for ROS and Δψ measurements, respectively. The fluorescence of $DIOC_6(3)$ was also measured in the presence of the uncoupling agent carbamoyl cyanide *m*-chlorophenylhydrazone (mClCCP) to confirm that fluorescence is correlated to Δψ.

Mitochondrial inner membrane potential was then monitored by flow cytometry using $DiOC_6(3)$ dye. The results showed a twofold decrease of the $\Delta\psi$ in the mutant strains compared to that of the wild type in both *rmp1* contexts (Table 3 and Figure S3). This indicates that there is no correlation between a reduction of the $\Delta\psi$ and mtDNA instability in the *PaAnt*^{M106P} and *PaAnt*^{A121P} mutants.

All the phenotypic defects caused by the *PaAnt* mutant alleles behave as dominant traits: The L98P, A114P, and V289M mutations are dominant in humans. To mimic the diploid organization of mammal somatic tissues and study whether the three alleles also behave as dominants in *P. anserina*, heteroallelic strains containing a mutant and a wild-type allele were constructed. The *PaAnt*$^{+}$ (*PaAnt*$^{+}$*-Hygro*) strain bearing a functional ectopic copy of the wild-type allele able to complement the deletion of the *PaAnt*$^{+}$ gene was crossed with the *PaAnt*^{M106P}, *PaAnt*^{A121P}, and *PaAnt*^{S296M} strains. The germination, growth rate, and longevity phenotypes of the three heteroallelic *PaAnt*^{M106P} (*PaAnt*$^{+}$), *PaAnt*^{A121P} (*PaAnt*$^{+}$), and *PaAnt*^{S296M} (*PaAnt*$^{+}$) strains were indistinguishable from the corresponding monoalleleic mutant strains (Table 1C). The presence of the wild-type allele did not modify the *rmp1* effect in the *PaAnt*^{M106P} and *PaAnt*^{A121P} strains or the premature death phenotype of the *PaAnt*^{S296M} strains irrespective of the *rmp1* allele present. As in homoallelic strains, death in *PaAnt*^{M106P} and *PaAnt*^{A121P} but not in *PaAnt*^{S296M} was accompanied by the accumulation of large-scale deletions affecting the same part of the mitochondrial genome without accumulation of senDNAα (data not shown). Importantly, the presence of the wild-type allele does not restore wild-type respiration rate, wild-type ROS production, or wild-type $\Delta\psi$ to the *PaAnt*^{M106P} and *PaAnt*^{A121P} strains (Table 3). Taken together, these data demonstrate that all the phenotypic traits due to the adPEO alleles behave as dominant traits in *P. anserina*.

DISCUSSION

In this study, we analyzed the properties of strains carrying three adPEO-associated missense mutations introduced into the *PaAnt* gene of *P. anserina*. The M106P, A121P, and S296M mutations in *P. anserina* correspond to the L98P, A114P (familial cases), and V289M (sporadic case) mutations of the *hANT1* gene in humans and to the M114P, A128P, and S303M mutations in *S. cerevisiae*. Alanine 114 and leucine 98 in the hANT1 protein map in highly conserved or conservatively substituted residues throughout eukaryotes, while valine 289 does not. The M114 and S303 residues of the *S. cerevisiae* Aac2 protein were replaced by their corresponding residues from the wild-type ANT1, resulting in "humanized wild type" *AAC2* alleles. These were functional and able to complement oxidative growth defects due to the *AAC2* deletion (Fontanesi *et al.* 2004).

The unique *PaAnt* gene is an essential gene: In contrast to humans and *S. cerevisiae*, in which several functional isoforms of the ADP/ATP translocator are present (Fiore *et al.* 1998; Dolce *et al.* 2005), only one gene has been found in *P. anserina* as in *N. crassa* (Arends and Sebald 1984) and numerous other filamentous fungi. Considering the central role of ATP/ADP transport across the mitochondrial inner membrane (MIM) in oxidative metabolism and the strict aerobic metabolism of *P. anserina*, it is not surprising that the *PaAnt* gene is essential. It is probable that the deletion of the ATP/ADP translocator results in ADP depletion in the mitochondrial matrix, which blocks the F_1-F_O ATPase and thus respiration. Also the absence of the most abundant inner membrane protein probably affects the structure of the inner membrane, which leads to respiration inhibition. Recently, it was demonstrated that in *S. cerevisiae* the abundant Aac2 isoform exists in physical interaction with the cytochrome bc_1-COX supercomplex and the TIM23 machinery and that, in the absence of Aac2, the assembly of the surpercomplex is altered (Dienhart and Stuart 2008).

Characteristics of the mtDNA instability distinguish between the severity of the three mutant alleles: In contrast to the Δ*PaAnt* allele, the three mutant alleles were viable but responsible for several detrimental effects on vegetative and sexual development, independently of the *rmp1* allele. These defects were more pronounced in the *PaAnt*^{S296M} mutant than in *PaAnt*^{M106P} and *PaAnt*^{A121P}. A reduced concentration of the mutant ANT protein was observed in the *PaAnt*^{M106P} and *PaAnt*^{A121P} strains. This could be due to a reduced import efficiency (De Marcos Lousa *et al.* 2002) or to a reduced stability of the mutant proteins. However, it seems unlikely that this reduction is responsible for the defects observed in the mutants since the mutations are dominant and the deletion of *PaAnt* is recessive (not shown) as is the deletion of *AAC2* in *S. cerevisiae* (Chen 2004). This strongly suggests that the mutant phenotypes are due to an alteration of, and not to a decreased amount of, mutant proteins.

In humans, the three adPEO mutations are linked to the formation of multiple mtDNA deletions (Kaukonen *et al.* 2000); in *S. cervisiae*, only *aac2*^{A128P} and *aac2*^{S303M}, but not *aac2*^{M114P}, were reported to cause an increase in abnormal mtDNA genomes (Fontanesi *et al.* 2004). In *P. anserina*, the three mutations are linked to the formation of large mitochondrial rearrangements. However, several properties differentiate *PaAnt*^{M106P} and *PaAnt*^{A121P} from the *PaAnt*^{S296M} mutation. First, in the *PaAnt*^{M106P} and *PaAnt*^{A121P} strains, the mitochondrial rearrangements correspond to large-scale mtDNA deletions covering a common region that represents ~60% of the genome with no identified fixed boundaries, whereas, in the *PaAnt*^{S296M} strain, they correspond to variable rearrangements and deletions involving different regions of the genome. Since in *P. anserina*,

mitochondrial instability leads to death, the timing of the death of a strain is an indicator of its mtDNA instability; it can therefore be concluded that the *PaAnt*^{S296M} allele causes greater mtDNA instability than either the *PaAnt*^{M106P} and the *PaAnt*^{A121P} allele.

A second difference is that the mtDNA instability caused by the *PaAnt*^{M106P}and the *PaAnt*^{A121P} mutations is observed in the presence of the *rmp1-1* allele and suppressed by the *rmp1-2* allele. In contrast, the *PaAnt*^{S296M} mutant showed huge mtDNA instability in the presence of either *rmp1* allele. Suppression of mtDNA instability by the *rmp1-2* allele has previously been reported in strains carrying the *AS1-4* allele, which alters a cytosolic ribosomal protein (Dequard-Chablat and Sellem 1994) and causes the accumulation of site-specific mtDNA deletions (Belcour *et al.* 1991; Contamine *et al.* 1996). The *rmp1-2* allele differs from *rmp1-1* by the presence of a nonsense mutation that eliminates the last 19 amino acids of the protein (Contamine *et al.* 2004). Thus *rmp1-1* is probably fully functional, and it could be directly or indirectly involved in the accumulation of large-scale deletions of the mtDNA genome such as those caused by the *AS1-4*, *PaAnt*^{M106P}, and *PaAnt*^{A121P} mutations, while the *rmp1-2* allele would delay the rate of accumulation of these deletions. In contrast, *rmp1* does not appear to be involved in the rate of accumulation of other types of mtDNA rearrangements such as those generated during senescence (senDNAs) or by the *PaAnt*^{S296M} mutation. *Rmp1* is an essential gene whose function is presently unknown. The encoded protein is localized in mitochondria and/or cytosol compartments depending on the cell type and the developmental stage. Putative homologs have been found only in filamentous fungi to date, but *rmp1* is thought to evolve rapidly, rendering the recognition of its homologs in other species very difficult (Contamine *et al.* 2004).

A third difference between the *PaAnt*^{M106P}/*PaAnt*^{A121P} and the *PaAnt*^{S296M} alleles is the synthetic phenotype obtained when *PaAnt*^{M106P} and *PaAnt*^{A121P} are associated with *AS1-4 rmp1-1*. The association of *PaAnt*^{M106P}/*PaAnt*^{A121P} but not *PaAnt*^{S296M} with *AS1-4 rmp1-1* leads to a spectacular stabilization of the mtDNA. A possible reason for the synthetic phenotype is that the deletions observed in *AS1-4 rmp1-1* and those observed in *PaAnt*^{M106P} *rmp1-1* and *PaAnt*^{A121P} *rmp1-1* are generated by mutually exclusive mechanisms.

Taken together, these results clearly show that the S296M mutation and the M106P/A121P mutations lead to different functional consequences. The predicted localization of the three *PaAnt* mutations derived from the crystal structure of the bovine ANT1 protein places the residues M106 and A121 in close proximity in the cytosolic gating region (Wang *et al.* 2008b), suggesting that the two mutations might induce similar structural changes. The S296M mutation is localized in a different region and thus may affect the translocator in a different and more severe manner, which may explain the particular properties of this mutation. These properties could also result from the sequence divergence between humans and *P. anserina* at this position (V289 in humans), which might suggest a specific role for this residue in *P. anserina*.

mtDNA instability is not systematically correlated with an increased ROS production or a reduced Δψ: Several mechanisms have been suggested to explain how the adPEO alleles of *hANT1* could lead to mtDNA instability: nucleotide imbalance causing defects in dATP biosynthesis and mtDNA replication (Kaukonen *et al.* 2000; Fontanesi *et al.* 2004); mtDNA damage by overproduction of ROS (Esposito *et al.* 1999; Palmieri *et al.* 2005); and the low Δψ model in which the pathogenic mutations uncouple the mitochondrial inner membrane primarily affecting mitochondrial biogenesis, which would have secondary effects on mtDNA stability (Chen 2002, 2004; Wang *et al.* 2008b). It was not possible to measure nucleotide exchange properties of the mutant strains because mitochondria isolated from these strains were of low quality, but it is presumed that a reduced availability of matrix ADP would inhibit the ATP synthase, causing hyperpolarization of the MIM and an increased production of ROS. This was demonstrated in tissues of *Ant1*-knockout mice (Esposito *et al.* 1999). In *S. cerevisiae*, the *aac2*^{A128P} and *aac2*^{M114P} alleles, corresponding to the *PaAnt*^{A121P} and *PaAnt*^{M106P} alleles, respectively, have been shown to uncouple the mitochondrial respiration and decrease the Δψ (Wang *et al.* 2008b). A more extensive study of *aac2*^{A128P} revealed that this allele is responsible for mitochondrial degeneration and degenerative cell death, probably due to the low Δψ. Interestingly, reduced cytosolic protein synthesis suppressed both membrane depolarization and mitochondrial degeneration, revealing a strong link between these two parameters (Wang *et al.* 2008a).

In *P. anserina*, the pathogenic mutations are responsible for defects in growth and sexual development, reduction of respiration rate, strong decline of the Δψ and of ROS production regardless of the *rmp1* allele, and mtDNA instability (and premature death) only in presence of the *rmp1-1* allele. The *rmp1-2* allele suppresses mtDNA instability (and therefore premature death) but not the other defects and is not accompanied by reestablishment of a wild-type Δψ. These results strongly suggest that, as already suggested for yeast (Wang *et al.* 2008a, b), the primary consequence of the adPEO-associated mutations is not the mtDNA instability but rather the damages to the electron transport chain which lead to growth and sexual development defects. These results also suggest that the decline of the Δψ alone is not sufficient to cause mtDNA instability and that other functions are implicated. The *rmp1-1* allele would have such a function, which would be lost for the *rmp1-2* allele that encodes a truncated protein.

All the traits associated with the adPEO alleles are dominant: Finally, it is of interest to note that all the phenotypes associated with *PaAnt*^{M106P} and *PaAnt*^{A121P} (and *PaAnt*^{S296M} when tested) are mediated by a dominant mechanism in *P. anserina* as in humans. These include slow growth rate, mitochondrial morphology modifications, mtDNA instability, timing of death, reduced respiration rate, reduced ROS production, and reduced $\Delta\psi$. The dominant nature of the three *PaAnt*^{M106P}, *PaAnt*^{A121P}, and *PaAnt*^{S296M} alleles strongly suggests that they correspond to a gain of function and that this function is deleterious for the cell. In *S. cerevisiae*, the three equivalent mutations behave as dominant for mtDNA instability and respiratory rate but recessive for oxidative growth (Fontanesi *et al.* 2004). In fact, it seems that at least for the equivalent A114P and L98P mutations, the dominant/recessive character of the mtDNA instability depends on the genetic balance between the mutated and the wild-type alleles (Wang *et al.* 2008b).

Taken together, the results presented in this work validate *P. anserina* as a model organism for studying the pathogenecity of different human mutations and underscore the importance of using a variety of model systems to dissect human mitochondrial disorders. They also show that, in *P. anserina*, the mtDNA instability associated with mitochondrial adenine translocator mutations is not due to increased ROS levels or to reduced $\Delta\psi$ alone. Thus, any proposed therapy increasing $\Delta\psi$ or limiting ROS production should be considered carefully. Finally, it is important to realize the central role of the genetic background in developing the pathogenic effects of a mutation.

We are very grateful to Carole Sellem for her constant interest in this work. We thank Sandrine Bach-Berkowicz for the construction of the vectors carrying the *PaAnt* mutant alleles and Edmund R. S. Kunji for his generous gift of the Aac2 monoclonal antibody. We thank Guy Lauquin and Véronique Trézéguet for useful discussions and critical comments, Vincent Rincheval for his help in the flow cytometry analysis, Chris Herbert and Linda Sperling for critical reading of the manuscript, and Delphine Petit for technical help. This work was supported by grants from the Association Française contre les Myopathies and the European Community's Sixth Framework Programme (LSHM-CT-200-512020).

LITERATURE CITED

Arends, H., and W. Sebald, 1984 Nucleotide sequence of the cloned mRNA and gene of the ADP/ATP carrier from *Neurospora crassa*. EMBO J. **3:** 377–382.

Bamber, L., D. Slotboom and E. R. S. Kunji, 2007 Yeast mitochondrial ADP/ATP carriers are monomeric in detergents as demonstrated by differential affinity purification. J. Mol. Biol. **371:** 388–395.

Begel, O., J. Boulay, B. Albert, E. Dufour and A. Sainsard-Chanet, 1999 Mitochondrial group II introns, cytochrome *c* oxidase, and senescence in *Podospora anserina*. Mol. Cell. Biol. **19:** 4093–4100.

Belcour, L., O. Begel and M. Picard, 1991 A site-specific deletion in mitochondrial DNA of Podospora is under the control of nuclear genes. Proc. Natl. Acad. Sci. USA **88:** 3579–3583.

Belcour, L., A. Sainsard-Chanet, C. Jamet-Vierny and M. Picard, 1999 Stability of the mitochondrial genome of *Podospora anserina* and its genetic control, pp. 209–228 in *Mitochondrial Diseases*, edited by P. Lestienne. Springer-Verlag, Berlin/New York.

Berges, T., and C. Barreau, 1989 Heat shock at an elevated temperature improves transformation efficiency of protoplasts from Podospora anserina. J. Gen. Microbiol. **139:** 601–604.

Borghouts, C., C. Q. Scheckhuber, A. Werner and H. D. Osiewacz, 2002 Respiration, copper availability and SOD activity in *P. anserina* strains with different lifespan. Biogerontology **3:** 143–153.

Chen, X. J., 2002 Induction of an unregulated channel by mutations in adenine nucleotide translocase suggests an explanation for human ophthalmoplegia. Hum. Mol. Genet. **11:** 1835–1843.

Chen, X. J., 2004 Sal1p, a calcium-dependent carrier protein that suppresses an essential cellular function associated with the Aac2 isoform of ADP/ATP translocase in *Saccharomyces cerevisiae*. Genetics **167:** 607–617.

Chinnery, F. P., 2003 Searching for nuclear-mitochondrial genes. Trends Genet. **19:** 60–62.

Contamine, V., G. Lecellier, L. Belcour and M. Picard, 1996 Premature death in *Podospora anserina*: sporadic accumulation of the deleted mitochondrial genome, translational parameters and innocuity of the mating types. Genetics **144:** 541–555.

Contamine, V. R., D. Zickler and M. Picard, 2004 The Podospora *rmp1* gene implicated in nucleus-mitochondria cross-talk encodes an essential protein whose subcellular location is developmentally regulated. Genetics **166:** 135–150.

Copeland, W. S., 2008 Inherited mitochondrial diseases of DNA replication. Annu. Rev. Med. **59:** 131–146.

Coppin, E., and R. Debuchy, 2000 Co-expression of the mating-type genes involved in internuclear recognition is lethal in *Podospora anserina*. Genetics **155:** 657–669.

Coppin-Raynal, E., 1981 Ribosomal suppressors and antisuppressors in *Podospora anserina*: altered susceptibility to paromomycin and relationships between genetic and phenotypic suppression. Biochem. Genet. **19:** 729–740.

Cummings, D. J., K. L. McNally, J. M. Domenico and E. T. Matsuura, 1990 The complete DNA sequence of the mitochondrial genome of *Podospora anserina*. Curr. Genet. **17:** 375–402.

De Marcos Lousa, C., V. Trezeguet, A.C. Dianoux, G. Brandolin and G.J. Lauquin, 2002 The human mitochondrial ADP/ATP carriers: kinetic properties and biogenesis of wild-type and mutant proteins in the yeast *S. cerevisiae*. Biochemistry **41:** 14412–14420.

Dequard-Chablat, M., and C. H. Sellem, 1994 The S12 ribosomal protein of *Podospora anserina* belongs to the S19 bacterial family and controls the mitochondrial genome integrity through cytoplasmic translation. J. Biol. Chem. **269:** 14951–14956.

Dienhart, M. K., and R. A. Stuart, 2008 The yeast Aac2 protein exists in physical association with the cytochrome bc_1-COX supercomplex and the TIM23 machinery. Mol. Biol. Cell. **19:** 3934–3943.

Dolce, V., P. Scarcia, D. Iacopetta and F. Palmieri, 2005 A fourth ADP/ATP carrier isoform in man: identification, bacterial expression, functional characterization and tissue distribution. FEBS Lett. **579:** 633–637.

Dufour, E., J. Boulay, V. Rincheval and A. Sainsard-Chanet, 2000 A causal link between respiration and senescence in *Podospora anserina*. Proc. Natl. Acad. Sci. USA **97:** 4138–4143.

El-Khoury, R., C. H. Sellem, E. Coppin, A. Boivin, M. F. Maas *et al.*, 2008 Gene deletion and allelic replacement in the filamentous fungus *Podospora anserina*. Curr. Genet. **53:** 249–258.

Espagne, E., O. Lespinet, F. Malagnac, C. Da Silva, O. Jaillon *et al.*, 2008 The genome sequence of the model ascomycete fungus *Podospora anserina*. Genome Biol. **9:** R77.

Esposito, L. A., S. Melov, A. Panov, B. A. Cottrell and D. C. Wallace, 1999 Mitochondrial disease in mouse results in increased oxidative stress. Proc. Natl. Acad. Sci. USA **96:** 4820–4825.

Esser, K., 1974 Podospora anserina, pp. 531–551 in *Handbook of Genetics*, edited by R. C. King. Plenum Press, New York.

Fiore, C., V. Trezeguet, A. Le Saux, P. Roux, C. Schwimmer *et al.*, 1998 The mitochondrial ADP/ATP carrier: structural, physiological and pathological aspects. Biochimie **80:** 137–150.

Fontanesi, F., L. Palmieri, P. Scarcia, T. Lodi, C. Donnini *et al.*, 2004 Mutations in AAC2, equivalent to human adPEO-associated

ANT1 mutations, lead to defective oxidative phosphorylation in *Saccharomyces cerevisiae* and affect mitochondrial DNA stability. Hum. Mol. Genet. **13:** 923–934.

Graham, B. H., K. G. Waymire, B. Cottrell, I. A. Trounce, G. R. MacGregor *et al.*, 1997 A mouse model for mitochondrial myopathy and cardiomyopathy resulting from a deficiency in the heart/muscle isoform of the adenine nucleotide translocator. Nat. Genet. **16:** 226–234.

Kaukonen, J., M. Zeviani, G. P. Comi, M. G. Piscaglia, L. Peltonen *et al.*, 1999 A third locus predisposing to multiple deletions of mtDNA in autosomal dominant progressive external ophthalmoplegia. Am. J. Hum. Genet. **65:** 256–261.

Kaukonen, J., J. K. Juselius, V. Tiranti, A. Kyttälä, M. Zeviani *et al.*, 2000 Role of adenine nucleotide translocator 1 in mtDNA maintenance. Science **289:** 782–785.

Klingenberg, M., 2008 The ADP and ATP transport in mitochondria and its carrier. Biochim. Biophys. Acta **1778:** 1978–2021.

Komaki, H., T. Fukazawa, H. Houzen, K. Yoshida, I. Nonaka *et al.*, 2002 A novel D104G mutation in the adenine nucleotide translocator 1 gene in autosomal dominant progressive external ophthalmoplegia patients with mitochondrial DNA with multiple deletions. Ann. Neurol. **51:** 645–648.

Lecellier, G., and P. Silar, 1994 Rapid methods for nucleic acids extraction from petri dish-grown mycelia. Curr. Genet. **25:** 122–123.

Lorin, S., E. Dufour, J. Boulay, O. Begel, S. Marsy *et al.*, 2001 Overexpression of the alternative oxidase restores senescence and fertility in a long-lived respiration-deficient mutant of *Podospora anserina*. Mol. Microbiol. **42:** 1259–1267.

Maxwell, D. P., Y. Wang and L. McIntosh, 1999 The alternative oxidase lowers mitochondrial reactive oxygen production in plant cells. Proc. Natl. Acad. Sci. USA **96:** 8271–8276.

Napoli, L., A. Bordoni, M. Zeviani, G. M. Hadjigeorgiou, M. Sciacco *et al.*, 2001 A novel missense adenine nucleotide translocator-1 gene mutation in a Greek adPEO family. Neurology **57:** 2295–2298.

Nury, H., C. Dahout-Gonzalez, V. Trezeguet, G. J. M. Lauquin, G. Brandolin *et al.*, 2006 Relations between structure and function of the mitochondrial ADP/ATP carrier. Annu. Rev. Biochem. **75:** 713–741.

Palmieri, F., 2004 The mitochondrial transporter family (SLC25): physiological and pathological implications. Pflugers Arch. **447:** 689–709.

Palmieri, L., S. Alberio, I. Pisano, T. Lodi, M. Meznaric-Petrusa *et al.*, 2005 Complete loss-of-function of the heart/muscle-specific adenine nucleotide translocator is associated with mitochondrial myopathy and cardiomyopathy. Hum. Mol. Genet. **14:** 3079–3088.

Riccio, P., H. Aquila and M. Klingenberg, 1975 Solubilization of the carboxy-atractylate binding protein from mitochondria. FEBS Lett. **56:** 192–232.

Rizet, G., 1952 Les phénomènes de barrage chez *Podospora anserina*. I. Analyse génétique des barrages entre souches S et s. Rev. Cytol. Biol. Vég. **13:** 51–92.

Sainsard-Chanet, A., O. Begel and Y. d'Aubenton-Carafa, 1998 Two co-existing mechanisms account for the large-scale deletions of mitochondrial DNA in *Podospora anserina* that involve the 5′ border of a group-II intron. Curr. Genet. **34:** 326–335.

Sellem, C. H., S. Marsy, A. Boivin, C. Lemaire and A. Sainsard-Chanet, 2007 A mutation in the gene encoding cytochrome *c1* leads to a decreased ROS content and to a long-lived phenotype in the filamentous fungus *Podospora anserina*. Fungal Genet. Biol. **44:** 648–658.

Siciliano, G., A. Tessa, S. Petrini, M. Mancuso, C. Bruno *et al.*, 2003 Autosomal dominant external ophthalmoplegia and bipolar affective disorder associated with a mutation in the ANT1 gene. Neuromuscul. Disord. **13:** 162–165.

Silar, P., 1995 Two new easy to use vectors for transformation. Fungal Genet. Newsl. 42: 73.

Silar, P., H. Lalucque and C. Vierny, 2001 Cell degeneration in the model system *Podospora anserina*. Biogerontology **2:** 1–17.

Stepien, G., A. Torroni, A. B. Chung, J. A. Hodge and D. C. Wallace, 1992 Differential expression of adenine nucleotide translocator isoforms in mammalian tissues and during muscle cell differentiation. J. Biol. Chem. **267:** 14592–14597.

Stumpferl, S. W., O. Stephan and H. D. Osiewacz, 2004 Impact of a disruption of a pathway delivering copper to mitochondria on *Podospora anserina* metabolism and life span. Eukaryot. Cell **3:** 200–211.

Wang, X., X. Zuo, B. Kucejova and X. J. Chen, 2008a Reduced cytosolic protein synthesis suppresses mitochondrial degeneration. Nat. Cell. Biol. **10:** 1090–1097.

Wang, X., K. Salinas, X. Zuo, B. Kucejova and X. J. Chen, 2008b Dominant membrane uncoupling by mutant adenine nucleotide translocase in mitochondrial diseases. Hum. Mol. Genet. **17:** 4036–4044.

Communicating editor: J. Engebrecht

GENETICS

Supporting Information
http://www.genetics.org/cgi/content/full/genetics.109.107813/DC1

Suppression of Mitochondrial DNA Instability of Autosomal Dominant Forms of Progressive External Ophthalmoplegia-Associated *ANT1* Mutations in *Podospora anserina*

Riyad El-Khoury and Annie Sainsard-Chanet

10.1534/genetics.109.107813

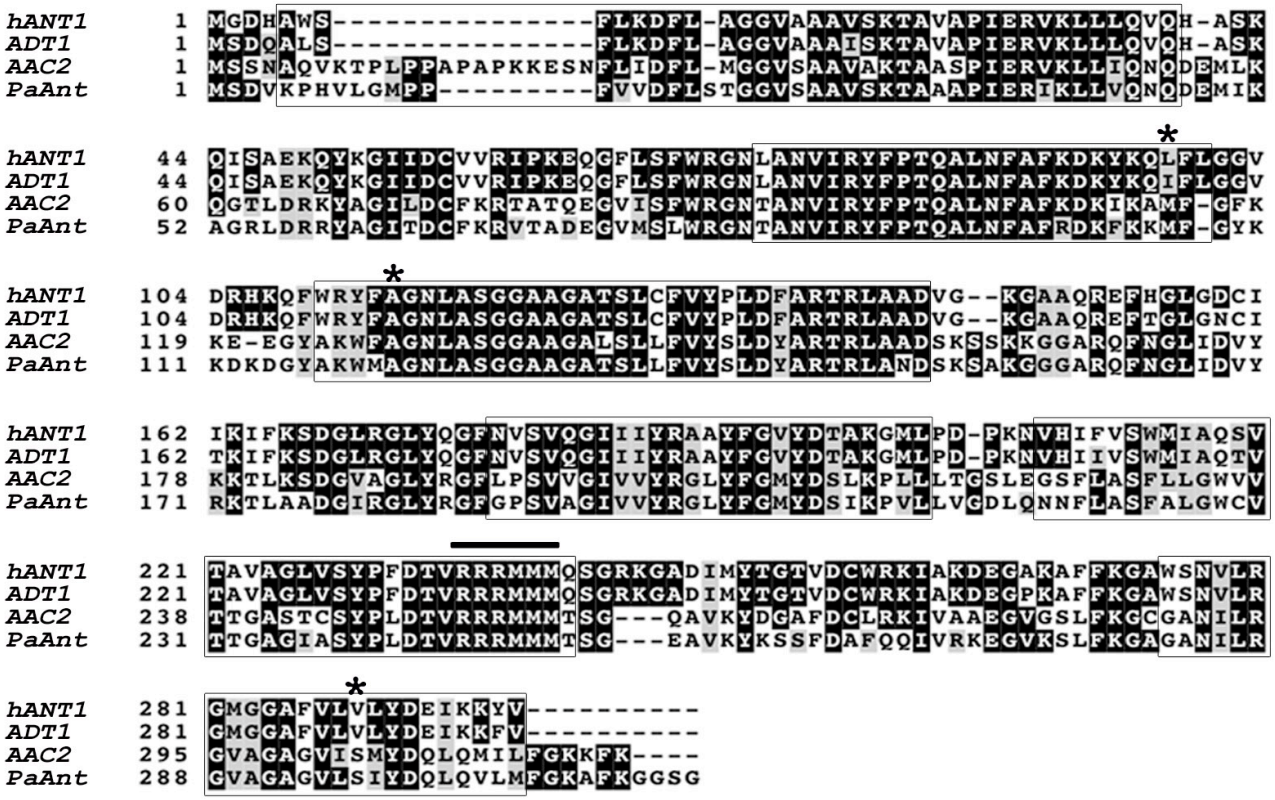

FIGURE S1.—Multiple sequence alignment of the amino acid sequences of the *H. sapiens* (hANT1), *B. taurus* (ADT1), *S. cerevisiae* (AAC2) and *P. anserina* (PaAnt) ADP/ATP translocators. The black horizontal bar corresponds to the consensus sequence RRRMMM. Stars correspond to the amino acids mutated in adPEO patients and their corresponding amino acids in the other species. Boxes define the six potential transmembrane segments based on that of *B. taurus*. The alignment was realized using the online software Clustal W version 1.4 with default parameters.

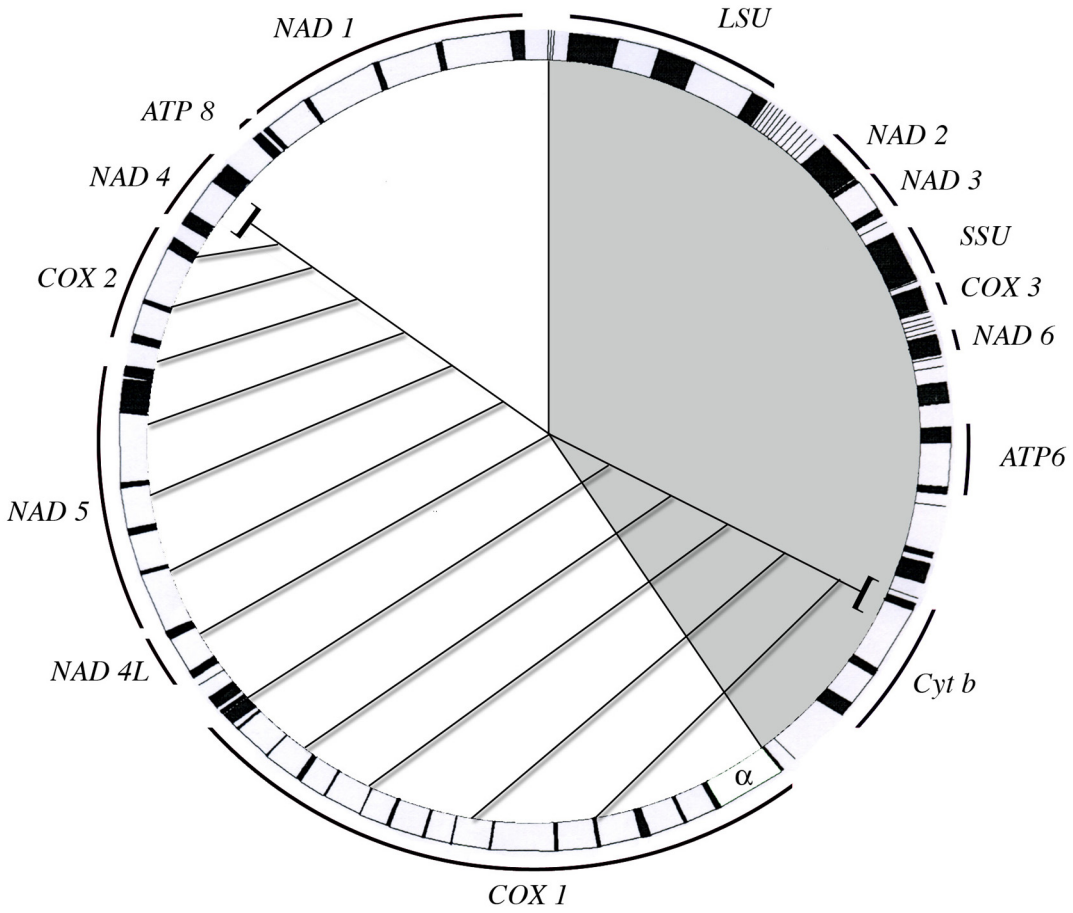

FIGURE S2.—Schematic representation of the mitochondrial chromosome of *P. anserina*. The size of the mitochondrial chromosome of *P. anserina*, race *s*, is 94 192 bp (CUMMINGS *et al.* 1990). The exons are presented in black, the introns in white. The bars represent tRNAs. LSU and SSU are the genes encoding the large and the small rRNAs, respectively. The other symbols are identical to those used for the homologous human genes. α corresponds to the first intron of gene *cox1* that gives senDNA during senescence. The grey part represents the deleted region in the dying *AS1-4 rmp1-1* strains (BELCOUR *et al.* 1991; SAINSARD-CHANET *et al.* 1998), the hatched part represents the deleted region in the dying *PaAnt*^{M106P} *rmp1-1* and *PaAnt*^{A121P} *rmp1-1* strains. The brakets at the extremities of the lines that delimit the deleted region in the *PaAnt*^{M106P} *rmp1-1* and *PaAnt*^{A121P} *rmp1-1* strains indicate that the boundaries of the deletions are imprecise.

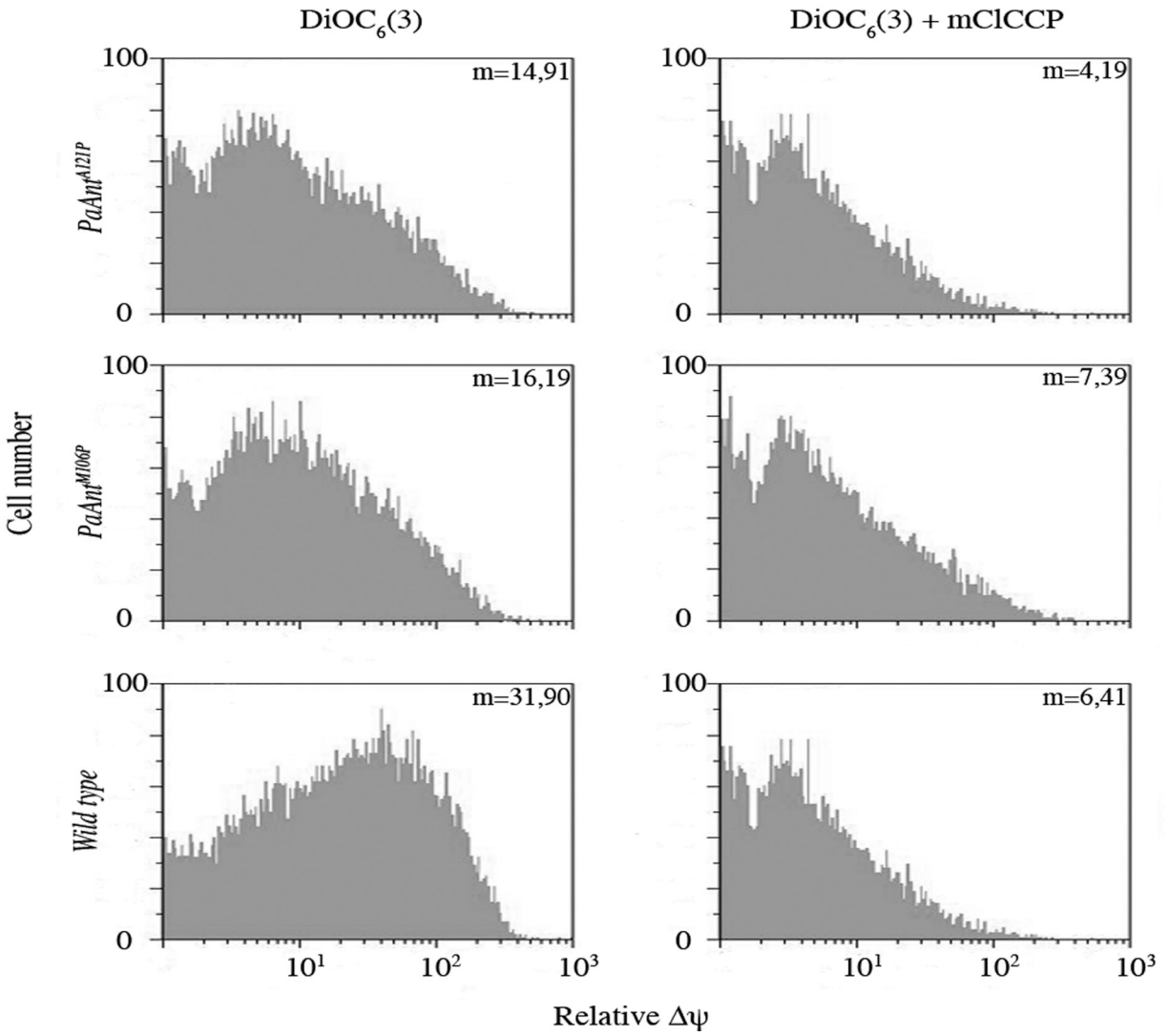

FIGURE S3.—Flow cytometry analysis of mitochondrial membrane potential ($\Delta\psi$). Measurement of the $\Delta\psi$ was based on the $\Delta\psi$-dependent uptake of the fluorescent dye $DiOC_6(3)$ in 50,000 protoplasts grown at 27° with or without the ionophore mClCCP that dissipates the mitochondrial membrane potential. Histograms representing measurements for the wild type, *PaAnt*^{M106P} *rmp1-2 mat+* and *PaAnt*^{A121P} *rmp1-2 mat+* mutant strains are shown. The same results were obtained in the *rmp1-1 mat-* context. The mean fluorescence value is indicated in each histogram. This value is then normalized to the quantity of the mitochondrial protein extracted from each strain.

TABLE S1

Primers used for site directed mutagenesis

Amino acid change	Oligonucleotides used (5' → 3')
M106P	M106P-F CGTGACAAGTTCAAGAAG**ccg**TTCGGCTACAAGAAGGAC
	M106P-R GTCCTTCTTGTAGCCGAA**cgg**CTTCTTGAACTTGTCACG
A121P	A121P-F GGCTACGCCAAGTGGATG**c**CTGGTAACCTTGCCTCCGGT
	A121P-R ACCGGAGGCAAGGTTACCAG**g**CATCCACTTGGCGTAGCC
S296M	S296M-F GCCGGTGCTGGTGTCTTG**atg**ATCTATGACCAGCTCCAG
	S296M-R CTGGAGCTGGTCATAGAT**cat**CAAGACACCAGCACCGGC

The modified nucleotides are shown in bold and lower case.